Annals of Nuclear Medicine
https://doi.org/10.1007/s12149-023-01858-5

ORIGINAL ARTICLE

Development of lung cancer risk prediction models based on F-18 FDG PET images

Kaeum Choi[1] · Jae Seok Park[2] · Yong Shik Kwon[2] · Sun Hyo Park[2] · Hyun Jung Kim[2] · Hyunju Noh[3] · Kyoung Sook Won[1] · Bong-Il Song[1] · Hae Won Kim[1]

Received: 6 April 2023 / Accepted: 9 July 2023

Abstract

Objective We aimed to evaluate whether the degree of F-18 fluorodeoxyglucose (FDG) uptake in the lungs is associated with an increased risk of lung cancer and to develop lung cancer risk prediction models using metabolic parameters on F-18 FDG positron emission tomography (PET).

Methods We retrospectively included 795 healthy individuals who underwent F-18 FDG PET/CT scans for a health check-up. Individuals who developed lung cancer within 5 years of the PET/CT scan were classified into the lung cancer group (n = 136); those who did not were classified into the control group (n = 659). The healthy individuals were then randomly assigned to either the training (n = 585) or validation sets (n = 210). Clinical factors including age, sex, body mass index (BMI), and smoking history were collected. The standardized uptake value ratio (SUVR) and metabolic heterogeneity (MH) index were obtained for the bilateral lungs. Logistic regression models including clinical factors, SUVR, and MH index were generated to quantify the probability of lung cancer development using a training set. The prediction models were validated using a validation set.

Results The lung SUVR and lung MH index in the lung cancer group were significantly higher than in the control group ($p < 0.001$ and $p < 0.001$, respectively). In the combined prediction model 1, age, sex, BMI, smoking history, and lung SUVR were significantly associated with lung cancer development (age: OR 1.07, $p < 0.001$; male: OR 2.08, $p = 0.015$; BMI: OR 0.93, $p = 0.057$; current or past smoker: OR 5.60, $p < 0.001$; lung SUVR: OR 1.13, $p < 0.001$). In the combined prediction model 2, age, sex, BMI, smoking history, and lung MH index showed a significant association with lung cancer development (age: OR 1.06, $p < 0.001$; male: OR 1.87, $p = 0.045$; BMI: OR 0.93, $p = 0.010$; current or past smoker: OR 4.78, $p < 0.001$; lung MH index: OR 1.33, $p < 0.001$). In the validation data, combined prediction models 1 and 2 exhibited very good discrimination [area under the receiver operator curve (AUC): 0.867 and 0.901, respectively].

Conclusions The metabolic parameters on F-18 FDG PET are related to an increased risk of lung cancer. Metabolic parameters can be used as biomarkers to provide information independent of the clinical parameters, related to lung cancer risk.

Keywords Prediction model · Lung cancer · F-18 FDG · PET · Cancer screening

Abbreviations

NLST	National Lung Screening Trial
FDG	Fluorodeoxyglucose (FDG)
PET	Positron emission tomography
BMI	Body mass index
ROI	Regions of interest
LUL	Left upper lobe
LLL	Left lower lobe
RUL	Right upper lobe
RML	Right middle lobe
RLL	Right lower lobe
SUVmax	Maximum standardized uptake value
SUVmin	Minimum SUV

Kaeum Choi and Jae Seok Park contributed equally to this work.

✉ Hae Won Kim
hwkim.nm@gmail.com

[1] Department of Nuclear Medicine, Keimyung University Dongsan Hospital, 1035 Dalgubeol-daero, Sindang-dong, Dalseo-gu, Daegu, Republic of Korea

[2] Department of Internal Medicine, Keimyung University Dongsan Hospital, Daegu, Republic of Korea

[3] Department of Nursing, Cheju Halla University, Cheju, Republic of Korea

Published online: 17 July 2023

SUVR	Standardized uptake value ratio
MH	Metabolic heterogeneity
ROC	Receiver operating characteristic
AUC	Area under the receiver operating characteristic curve

Introduction

Lung cancer is the leading cause of cancer-related death worldwide [1]. According to the National Lung Screening Trial (NLST) results, medical organizations have recommended annual CT lung cancer screening in high-risk individuals aged 55–74 years who have a 30 pack-year smoking history and currently smoke or have quit within 15 years [2]. However, low-dose CT screening reveals a large number of indeterminate nodules, and < 50% of patients with lung cancer are eligible for screening [3]. In addition, major concerns regarding annual low-dose CT screening include additional medical costs due to a large number of false-positive results and the harm caused by excessive radiation exposure from repeated CT scans [4]. Thus, selective low-dose CT screening in individuals with a higher risk of lung cancer is expected to improve the cost-effectiveness and reduce harm.

In the pathophysiology of lung cancer, it is now evident that chronic inflammation is involved in all stages of lung cancer development, from malignant transformation and tumor initiation to invasion and metastasis [5]. Persistent exposure to several exogenous factors, including smoking, asbestos, radiation, and air pollution, increases the risk of chronic inflammation and consequently induces lung cancer development in combination with genetic factors [6]. From the viewpoint of lung cancer pathophysiology with chronic pulmonary inflammation, F-18 fluorodeoxyglucose (FDG) positron emission tomography (PET) can provide additional information to identify individuals with a higher risk of lung cancer because it can be used to noninvasively evaluate the inflammatory activity in the body [7]. In particular, F-18 FDG PET can serve as a surrogate marker of pulmonary inflammation [8].

Thus, it is postulated that the specific pattern of F-18 FDG uptake in the lungs, indicating chronic pulmonary inflammation, can be used to predict lung cancer development. The aim of the present study was to evaluate whether the degree of F-18 FDG uptake in the lungs is associated with an increased risk of lung cancer, and to develop lung cancer risk prediction models using metabolic parameters on F-18 FDG PET.

Material and methods

Study population

This retrospective study included healthy individuals who underwent initial F-18 FDG PET/CT scans for a health check-up at our institution between January 2008 and December 2016; we confirmed no evidence of lung cancer or other malignancies. Individuals who met the following criteria were excluded: no follow-up chest CT or PET/CT after 5 years of the initial PET/CT; no medical record of smoking history or body mass index (BMI); and history of acute infection. Individuals who developed lung cancer within 5 years of the initial PET/CT scan were classified into the lung cancer group. The development of lung cancer was defined based on the follow-up chest CT or PET/CT scans, and confirmed by pathological results. Individuals who did not develop lung cancer within 5 years after the initial PET/CT scan were classified into the control group. Clinical factors including age, sex, BMI, and smoking history (never, past, or current smoker) were collected for all patients. The healthy individuals were then randomly assigned to either the training or validation sets. This study was approved by the Institutional Review Board of our institution.

F-18 FDG PET/CT images

A PET/CT system (Discovery STE 16, GE Healthcare, Milwaukee, WI, USA) was used to acquire torso F-18 FDG PET images, as previously described [9]. Patients received intravenous administration of 7.0 MBq/kg F-18 FDG. Images were acquired 60 min after F-18 FDG administration. A non-contrast CT scan was performed for attenuation correction and localization. Immediately after the CT scan, PET images were acquired from the base of the skull or the top of the brain to the proximal thigh.

To develop the risk prediction model, an experienced nuclear medicine physician (H.W.K.) reviewed all F-18 FDG PET images using a dedicated workstation (Advantage Workstation version 4.3; GE Healthcare). Two-dimensional regions of interest (ROIs) (long-axis diameter range, 10 mm) were drawn on the pulmonary parenchyma in the left upper lobe (LUL), left lower lobe (LLL), right upper lobe (RUL), right middle lobe (RML), and right lower lobe (RLL) of the lung, as well as the blood pool of the aortic arch (Fig. 1). The ROIs included chronic inflammatory changes such as emphysematous changes, while excluding pulmonary nodules, vascular structures, active inflammation, and bullae. For each lobe of the bilateral lungs, the maximum standardized uptake value (SUVmax), mean SUV (SUVmean), and minimum SUV (SUVmin) were obtained. The SUV ratio (SUVR) and metabolic heterogeneity (MH) index were calculated as follows: SUVR = (SUVmax of lung parenchyma/SUVmax of blood pool) × 100; MH index = [(SUVmax of lung parenchyma − SUVmin of lung parenchyma)/SUVmax of blood pool)] × 100, according to a previously validated method [10]. The lung SUVmax, SUVmean, SUVmin, SUVR, and MH index were defined as the respective average values for each lobe. In addition, an ROI (long-axis diameter

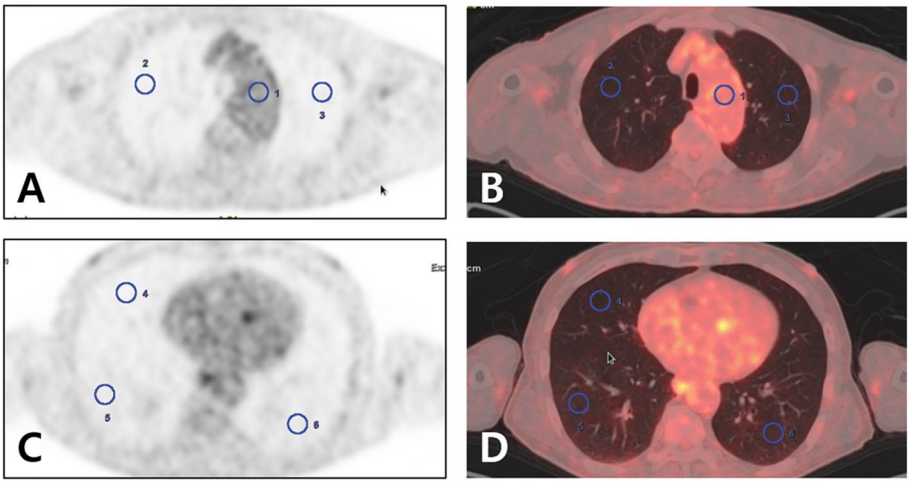

Fig. 1 Representative images of regions of interest (ROIs) for calculating the metabolic parameters. Two-dimensional ROIs were drawn on the blood pool of the aortic arch and the pulmonary parenchyma in the right upper lobe and left upper lobe of the lung (**a**, **b**). The ROIs also were drawn on the pulmonary parenchyma in the right middle lobe, right lower lobe, and left lower lobe of the lung (**c**, **d**)

range, 10 mm) was drawn on the central area of the right hepatic lobe, to obtain the liver SUVmax, SUVmean, and SUVmin. To assess inter-observer reproducibility, one another experienced nuclear medicine physician (K.S.W.) reviewed the F-18 FDG PET images of 100 randomly selected participants in the training set. The ROIs of the bilateral lungs were delineated using the same methodology as in the development of the risk prediction model, and the lung SUVmax, SUVmean, SUVmin, SUVR, and MH index were calculated accordingly.

Development of the risk prediction model

The prediction models were configured to estimate the absolute risk that an individual would have lung cancer in 5 years. Logistic regression models to quantify the probability of lung cancer development were generated using the training data set. Simple prediction models were constructed, including only clinical factors (age, sex, BMI, and smoking history) or only metabolic parameters (lung SUVR and lung MH index). Combined prediction models, including clinical factors and metabolic parameters, were also constructed. The combined prediction model 1 included all variables in the clinical model and lung SUVR. In the combined prediction model 2, all variables in the clinical model and the lung MH index were included. The β coefficients from the logistic regression models were used to create the prediction model: probability $= e^k/(1+e^k)$, where $k = \beta_0 + \beta_1 X_1 + \beta_2 X_2 + \cdots + \beta_n X_n$.

Validation of the risk prediction model

The prediction models were validated using the validation data set. The performance of the prediction models was evaluated using C-statistics with respect to discrimination. The C-statistic, also called the receiver operating characteristic (ROC) curve, is a measure of goodness of fit for binary outcomes in a logistic regression model [11]. The prediction model was considered good when the area under the ROC curve (AUC) was over 0.70 and very good when the AUC was over 0.80 [12]. The performance of the prediction models was also evaluated using the Brier score with respect to calibration. Calibration numerically represents how closely the predicted probabilities match the actual outcomes. The risk of developing lung cancer for each participant was calculated, and the average predicted probabilities were compared with the actual probabilities of developing lung cancer in each decile. The Brier score was calculated as the mean squared difference between the predicted and actual outcome. A Brier score of 0 indicates perfect accuracy.

Statistical analysis

All statistical analyses were conducted using SPSS for Windows, version 25.0 (IBM Corp., Armonk, NY, USA). Pearson's correlation analysis was employed to assess the associations between metabolic parameters, including SUVmax, SUVmean, SUVmin, SUVR, and MH index, with age or BMI. Two-sample t-tests were utilized to compare all metabolic parameters for the lung, liver, and blood pool, between male and female groups, smoker and non-smoker groups, as well as control and lung cancer groups. Paired sample t-tests were performed to compare metabolic parameters among each lobe of the bilateral lungs. Univariate and multivariate logistic regression models, incorporating both metabolic parameters and clinical factors, were utilized for the development of the risk prediction model. Inter-observer reproducibility was assessed using the coefficient of variation (CV) between the two observers. A CV of 15% or lower was considered indicative of good reproducibility [13]. Variables with p-values < 0.05 from the univariate analysis were included in the subsequent multivariate regression analysis. A p-value < 0.05 was considered statistically significant.

Results

Characteristics

A total of 795 participants from our institution were enrolled in this study. Of these, 136 developed lung cancer within 5 years of the initial PET/CT scan. Among the participants with lung cancer development, the most prevalent histologic type was adenocarcinoma (47.1%), followed by squamous carcinoma (41.2%), and small cell carcinoma (8.8%) (Supplementary Table 1). Furthermore, of the 795 participants, 585 and 210 were randomly assigned to the training and validation data sets, respectively (Fig. 2). In the training set, 100 out of 585 participants developed lung cancer within 5 years of the initial F-18 FDG PET/CT scans and were classified into the lung cancer group. Table 1 shows the characteristics of the participants included in the training set. In the validation set, 36 out of 210 participants developed lung cancer within 5 years of the initial F-18 FDG PET/CT scans and were classified into the lung cancer group. The characteristics of the validation sets are listed in Supplementary Table 2.

The lung SUVR showed a significantly positive correlation with age ($r = 0.165$, $p < 0.001$). However, there were no significant associations between age and SUVmax, SUVmean, SUVmin, and MH index ($p = 0.077$, $p = 0.447$, $p = 0.321$, and $p = 0.174$, respectively). There were positive associations between BMI and the lung SUVmax, SUVmean, SUVmin, and MH index ($r = 0.492$, $p < 0.001$; $r = 0.471$, $p < 0.001$; $r = 0.415$, $p < 0.001$; $r = 0.373$, $p < 0.001$, respectively), but no significant association between BMI and the lung SUVR ($p = 0.059$). The lung SUVmean, SUVmin, and MH index were significantly

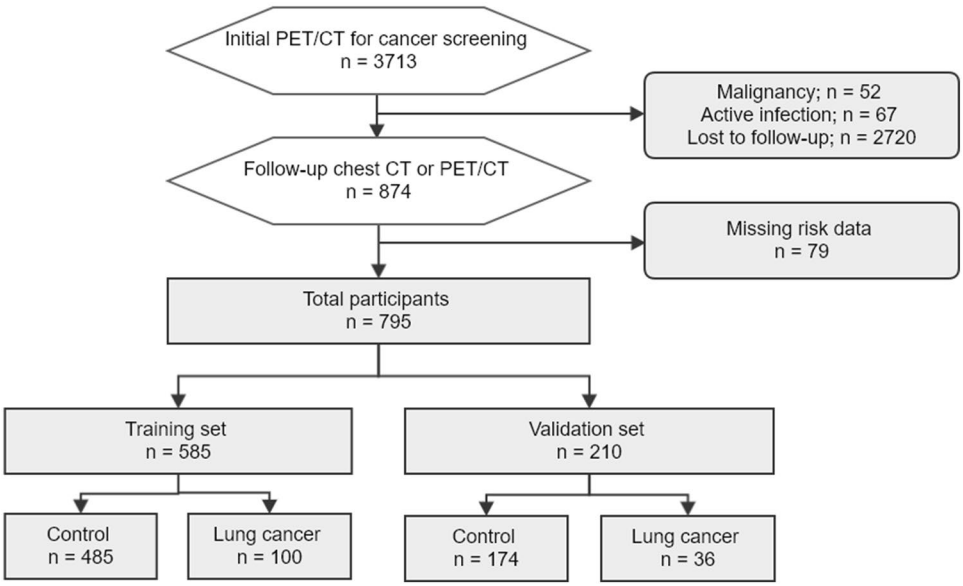

Fig. 2 Flow diagram of the training and validation data sets. *PET* positron emission tomography, *CT* computed tomography

Table 1 Baseline characteristics and univariate analysis results for the training set

Risk factor	Control (n = 485)	Lung cancer (n = 100)	OR (95% CI)	*p* value
Age, years (SD)	60.3 (11.9)	69.2 (9.4)	1.08 (1.05–1.11)	< 0.001
Male, *n*, (%)	176 (36.3)	73 (73.0)	4.75 (2.94–7.66)	< 0.001
Body mass index (SD)	23.7 (3.6)	22.9 (3.4)	0.94 (0.88–1.00)	0.051
Current or past smoker, *n*, (%)	181 (37.3)	77 (77.0)	5.62 (3.41–9.28)	< 0.001
Lung SUVmax (SD)	0.59 (0.11)	0.69 (0.15)	1113.42 (153.80–8060.60)	< 0.001
Lung SUVmean (SD)	0.45 (0.09)	0.50 (0.11)	347.52 (34.42–3508.34)	< 0.001
Lung SUVmin (SD)	0.35 (0.08)	0.37 (0.09)	31.67 (2.07–484.26)	0.013
Lung SUVR (SD)	28.48 (9.13)	37.0 (9.89)	1.12 (1.09–1.16)	< 0.001
Lung MH index (SD)	11.76 (3.99)	17.45 (6.02)	1.38 (1.28–1.48)	< 0.001

OR odds ratio, *SD* standard deviation, *SUVmax* maximum standardized uptake value, *SUVmean* mean standardized uptake value, *SUVmin* minimum standardized uptake value, *SUVR* standardized uptake value ratio, *MH index* metabolic heterogeneity index

higher in the female group compared to those in the male group (0.47 ± 0.09 vs. 0.44 ± 0.11, $p = 0.007$; 0.36 ± 0.07 vs. 0.33 ± 0.08, $p < 0.001$; 12.32 ± 4.66 vs. 13.29 ± 5.15, $p = 0.018$, respectively), but there were no differences in the lung SUVmax and SUVR between the female and male groups ($p = 0.073$ and $p = 0.973$). The lung SUVmean and SUVmin were significantly lower in the current or past smoker group compared to the non-smoker group (0.46 ± 0.09 vs. 0.45 ± 0.10, $p = 0.027$ and 0.36 ± 0.08 vs. 0.34 ± 0.08, $p < 0.001$), but there were no differences in the lung SUVmax, SUVR, and MH index between the current or past smoker and non-smoker groups ($p = 0.434$, $p = 0.505$, and $p = 0.076$, respectively). When comparing metabolic parameters between the lobes of the bilateral lungs, all metabolic parameters including SUVmax, SUVmean, SUVmin, SUVR, and MH index were significantly higher in the RLL compared to those in the RUL or RML ($p < 0.001$ and $p < 0.001$, respectively). In the left lung, all metabolic parameters were significantly higher for the LLL than for the LUL ($p < 0.001$) (Supplementary Table 3). The inter-observer CV for all metabolic parameters ranged from 2.7% to 5.3% in the randomly selected 100 participants of the training set, indicating good reproducibility. Specifically, the CVs for SUVmax, SUVmean, SUVmin, SUVR, and MH index were 4.3%, 5.3%, 4.2%, 2.8%, and 3.8%, respectively. The measurements of SUVmax, SUVmean, SUVmin, SUVR, and MH index in the 100 randomly selected participants are presented in Supplementary Table 4.

Risk prediction model

In the univariate analysis, age, sex, smoking history, lung SUVmax, SUVmean, SUVmin, SUVR, and MH index were significantly associated with lung cancer development ($p < 0.001$, $p < 0.001$, $p = 0.013$ $p < 0.001$ and $p < 0.001$, respectively) (Table 1). In the lung cancer group, lung SUVmax, SUVmean, SUVmin, SUVR, and MH index were significantly higher than those in the control group ($p < 0.001$, $p < 0.001$, $p = 0.012$ $p < 0.001$ and $p < 0.001$, respectively). The lung SUVmax, SUVmean, SUVmin, SUVR, and MH index for most of the lobes in the lung cancer group were significantly higher than those in the control group (Table 2). All the metabolic parameters in the blood pool and liver were not significantly different between the control and lung cancer groups (Supplementary Table 5).

In the multivariate analysis, only the lung SUVR and MH index, which were better calibrated than the lung SUVmax, SUVmean and SUVmin, were considered. The clinical model included age, sex, BMI, and smoking history, and age, sex and smoking history were significantly associated with lung cancer development (age: OR 1.07, $p < 0.001$; male: OR 2.13, $p = 0.006$; past or current smoker: OR 4.60, $p < 0.001$). In the combined prediction model 1, all variables in the clinical model and lung SUVR were included, and age, sex, BMI, smoking history, and lung SUVR were significantly associated with lung cancer development (age: OR 1.07, $p < 0.001$; male: OR 2.08, $p = 0.015$; BMI: OR 0.93, $p = 0.057$; current or past smoker: OR 5.60, $p < 0.001$; lung SUVR: OR 1.13, $p < 0.001$). In the combined prediction model 2, all variables in the clinical model and lung MH index were included, and age, sex, BMI, smoking history, and lung MH index showed a significant association with lung cancer development (age: OR 1.06, $p < 0.001$; male: OR 1.87, $p = 0.045$; BMI: OR 0.93, $p = 0.010$; current or past smoker: OR 4.78, $p < 0.001$; lung MH index: OR 1.33, $p < 0.001$) (Table 3).

Table 2 Comparison of metabolic parameters between the control and lung cancer groups

Region	Parameter	Control	Lung cancer	*p* value
Lung	SUVmax	0.59 (0.11)	0.70 (0.15)	< 0.001
	SUVmean	0.45 (0.09)	0.50 (0.11)	< 0.001
	SUVmin	0.35 (0.08)	0.37 (0.09)	0.012
	SUVR	28.48 (9.13)	37.02 (9.89)	< 0.001
	MH index	11.76 (3.99)	17.45 (6.02)	< 0.001
RUL	SUVmax	0.54 (0.12)	0.62 (0.20)	< 0.001
	SUVmean	0.40 (0.09)	0.44 (0.14)	0.002
	SUVmin	0.31 (0.08)	0.32 (0.10)	0.292
	SUVR	25.73 (8.28)	32.72 (11.15)	< 0.001
	MH index	10.92 (4.22)	15.93 (7.03)	< 0.001
RML	SUVmax	0.50 (0.12)	0.56 (0.16)	< 0.001
	SUVmean	0.37 (0.09)	0.39 (0.11)	0.053
	SUVmin	0.28 (0.08)	0.28 (0.08)	0.543
	SUVR	24.19 (11.22)	29.79 (9.83)	< 0.001
	MH index	10.49 (6.96)	14.97 (7.19)	< 0.001
RLL	SUVmax	0.70 (0.14)	0.81 (0.20)	< 0.001
	SUVmean	0.54 (0.11)	0.61 (0.14)	< 0.001
	SUVmin	0.43 (0.10)	0.45 (0.12)	0.053
	SUVR	33.48 (10.47)	43.61 (13.37)	0.007
	MH index	12.90 (4.80)	19.33 (7.77)	< 0.001
LUL	SUVmax	0.56 (0.13)	0.65 (0.19)	< 0.001
	SUVmean	0.41 (0.10)	0.45 (0.13)	0.002
	SUVmin	0.32 (0.08)	0.32 (0.10)	0.624
	SUVR	26.66 (9.23)	34.12 (10.93)	< 0.001
	MH index	11.34(4.68)	17.33 (8.44)	< 0.001
LLL	SUVmax	0.67 (0.15)	0.85 (0.17)	< 0.001
	SUVmean	0.51 (0.13)	0.62 (0.14)	< 0.001
	SUVmin	0.40 (0.11)	0.48 (0.12)	< 0.001
	SUVR	32.34 (10.53)	45.39 (11.54)	< 0.001
	MH index	13.14 (4.84)	19.93 (7.30)	< 0.001

RUL right upper lobe, *RML* right middle lobe, *RLL* right lower lobe, *LUL* left upper lobe, *LLL* left lower lobe, *SUVmax* maximum standardized uptake value, *SUVmean* mean standardized uptake value, *SUVmin* minimum standardized uptake value, *SUVR* standardized uptake value ratio, *MH index* metabolic heterogeneity index

Validation of the risk prediction model

In the validation data, the clinical model had an AUC of 0.798 and a Brier score of 0.119. The simple prediction model with SUVR had an AUC of 0.681 and a Brier score of 0.131, while a simple prediction model with an MH index had an AUC of 0.825 and a Brier score of 0.125. There was no significant difference in the AUC between the simple prediction model with SUVR or MH index, and the clinical model ($p = 0.058$ and $p = 0.657$). The combined prediction model 1 with clinical factors and SUVR had better performance than the clinical model ($p = 0.030$), with an AUC of 0.867 and Brier score of 0.100. The combined prediction model 2 with clinical factors and the MH index also had better performance than the clinical model ($p = 0.001$), with an AUC of 0.901 and Brier score of 0.100 (Figs. 3, 4). The AUC and Brier scores for each prediction model are displayed in Table 4. The sensitivity, specificity, positive predictive value, negative predictive value, accuracy, and AUC of each prediction model for lung cancer development using 5%, 10%, 20%, 30%, 40% and 50% probability of lung cancer development are listed in Supplementary Table 6.

Table 3 Multivariable logistic regression model for the prediction of lung cancer development in the training set

Clinical model	Standardized β	OR (95%CI)	p value
Age, years	0.07	1.07 (1.04–1.09)	< 0.001
Male	0.75	2.13 (1.24–3.64)	0.006
Body mass index	–	–	0.167
Past or current smoker	1.53	4.60 (2.67–7.93)	< 0.001
AUC		0.803 (0.752–0.853)	
Brier score		0.111 (0.092–0.130)	
Combined model 1			
Age, years	0.07	1.07 (1.04–1.10)	< 0.001
Male	0.73	2.08 (1.15–3.77)	0.015
Body mass index	− 0.08	0.93 (0.85–1.00)	0.057
Past or current smoker	1.72	5.60 (3.04–10.31)	< 0.001
Lung SUVR	0.12	1.13 (1.09–1.17)	< 0.001
AUC		0.885 (0.844–0.925)	
Brier score		0.082 (0.065–0.099)	
Combined model 2			
Age, years	0.06	1.06 (1.03–1.09)	< 0.001
Male	0.63	1.87 (1.02–3.44)	0.045
Body mass index	− 0.07	0.93 (0.86–1.01)	0.010
Past or current smoker	1.56	4.78 (2.57–8.89)	< 0.001
Lung MH index	0.28	1.33 (1.23–1.43)	< 0.001
AUC		0.897 (0.858–0.936)	
Brier score		0.077 (0.061–0.094)	

OR odds ratio, *AUC* area under the receiver-operator curve, *SUVR* standardized uptake value ratio, *MH index* metabolic heterogeneity index

Discussion

The present study developed risk prediction models for lung cancer development using F-18 FDG PET images. The F-18 FDG uptake and metabolic heterogeneity on F-18 FDG PET images were higher in the lung cancer group than in the control group, demonstrating that chronic inflammation of the lungs is associated with the development of lung cancer. Age, sex, smoking history, BMI, and metabolic parameters were significant risk factors for lung cancer in developing prediction models. The validation result showed that these prediction models successfully distinguished between high-risk and low-risk individuals for lung cancer. The present study is the first to use F-18 FDG PET to evaluate the risk of lung cancer.

It is now evident that chronic pulmonary inflammation is involved in the tumorigenesis of lung cancer, from malignant transformation and tumor initiation to invasion and metastasis [5]. Inflammatory airway injuries resulting from smoking, a variety of occupational agents, or indoor and outdoor air pollution induce cell proliferation, apoptosis resistance, inflammation, and DNA alterations that lead to lung cancer [14]. Chronic pulmonary infections and inflammatory lung diseases such as asthma, chronic obstructive

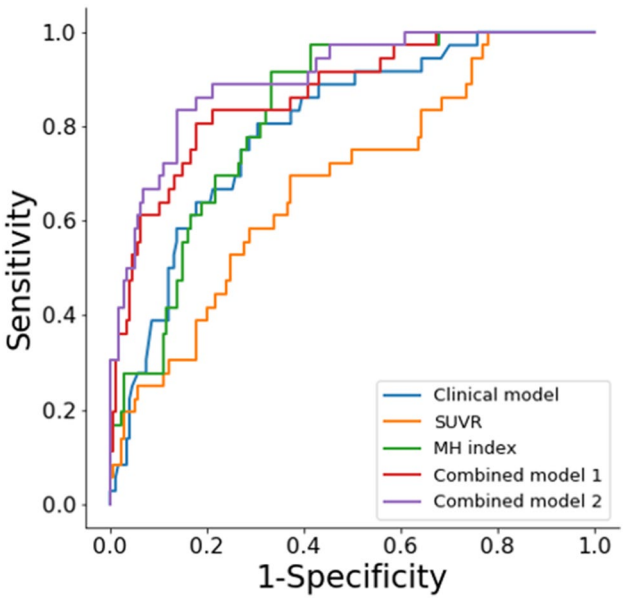

Fig. 3 ROC curves for the clinical model, simple model with SUVR, simple model with the MH index, combined model 1 with clinical factors and SUVR, and combined model 2 with clinical factors and the MH index. *ROC* receiver operating characteristic, *SUVR* standardized uptake value ratio, *MH* metabolic heterogeneity

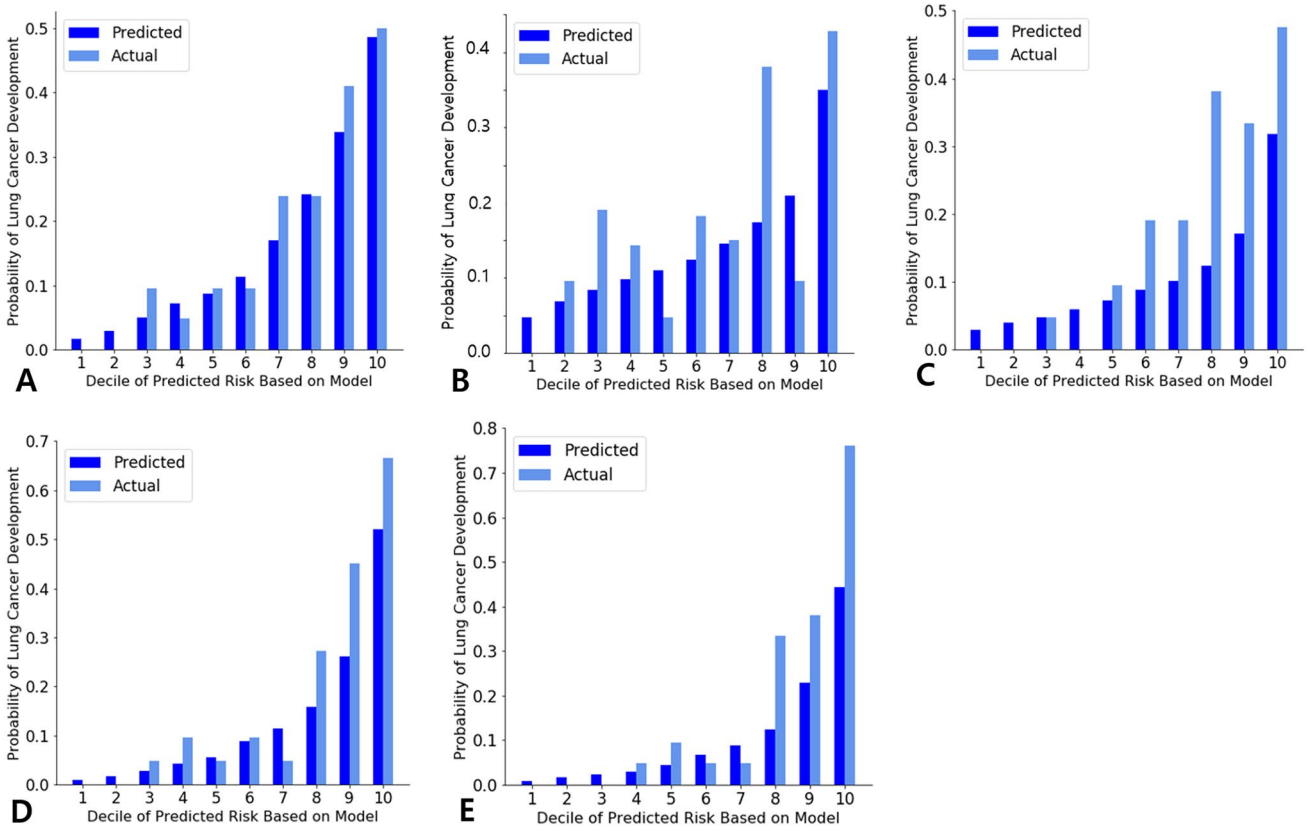

Fig. 4 Calibration of the lung cancer prediction models tested on the validation set. **a** Calibration of clinical model, **b** Calibration of lung SUVR, **c** Calibration of lung MH index, **d** Calibration of combined model 1, **e** Calibration of combined model 2. *SUVR* standardized uptake value ratio, *MH* metabolic heterogeneity

Table 4 Performance of the lung cancer prediction models

Prediction model	AUC (95% CI)	Brier score (95% CI)
Clinical model	0.798 (0.725–0.872)	0.119 (0.086–0.153)
Lung SUVR	0.681 (0.587–0.775)	0.131 (0.097–0.166)
Lung MH index	0.825 (0.763–0.887)	0.125 (0.091–0.159)
Combined model 1	0.867 (0.802–0.931)	0.100 (0.069–0.132)
Combined model 2	0.901 (0.848–0.954)	0.100 (0.069–0.131)

OR odds ratio, *AUC* area under the receiver-operator curve, *SUVR* standardized uptake value ratio, *MH index* metabolic heterogeneity index

pulmonary disease, and fibrosis are also associated with an increased risk of lung cancer [15]. However, since not all individuals with these risk factors develop lung cancer via chronic pulmonary inflammation, there is a limit to predicting lung cancer development with these risk factors based on epidemiological data. From this point of view, F-18 FDG PET can provide information on the risk of lung cancer based on the fact that the pathophysiology of lung cancer is associated with chronic pulmonary inflammation [16]. This is because activated neutrophils and macrophages in the lung promote increased F-18 FDG uptake with increasing pulmonary inflammation [17]. Several studies have demonstrated the usefulness of F-18 FDG PET in measuring inflammatory activity in various organs, such as the lungs, arteries, bones, and intestines [7]. In the present study, it was observed that all the metabolic parameters, including the SUVmax, SUVmean, SUVmin, SUVR, and MH index, in the RLL or LLL were significantly higher compared to those in the RUL or LUL. These findings are believed to be attributed to the impact of inflammatory lung diseases, such as COPD and emphysema, which predominantly affect the lower regions of the lungs, leading to the destruction of the alveoli in those areas [18]. Therefore, these findings suggest that the metabolic parameters based on F-18 FDG PET reflect the inflammatory activities in the lungs effectively. Furthermore, in the present study, we found that all metabolic parameters were higher in the high-risk individuals for lung cancer than in those with a low-risk, and demonstrated that the metabolic parameters are associated with an increased risk of lung cancer development.

Various semiquantitative parameters can be evaluated using F-18 FDG PET, including the SUVmax, SUVmean, SUVmin, SUVR, and MH index [19]. The SUV, defined as

the F-18 FDG concentration at a certain time point normalized to the injected dose per unit body weight, has been generally used to measure the degree of pulmonary inflammation [8]. However, despite its proven role in the diagnosis and staging of lung cancer or other malignancies, it has limitations in consistently and accurately evaluating the metabolic rate from person to person because it is a static imaging procedure measured at a single time point and is affected by various patient-related and technical factors [20]. In particular, the semiquantitative parameter using SUV to measure lung parenchyma with a low metabolic rate, rather than measuring a target with a high metabolic rate, such as a tumor, can greatly affect results even with a small error in the comparison of the metabolic rate [21]. Furthermore, in the present study, the lung SUV values were often on a small scale, and their mean values yielded high odds ratios in logistic regression analyses. When an independent variable has a small scale, such as the lung SUVmax, SUVmean, and SUVmin, even a slight change in their values can lead to substantial odds ratio changes [22]. However, it is important to note that such large odds ratios may not necessarily reflect realistic variable changes, as actual changes in practice tend to be small. To address these limitations associated with SUV, we considered using the lung SUVR. The SUVR, defined as the target-to-blood pool F-18 FDG uptake ratio, has been frequently used in neuroreceptor imaging and in oncology, and has been recognized as an alternative to SUV [23]. The use of SUVR eliminates the shortcomings of the SUV because SUVR is a dimensionless quantity that is neither affected by scanner inaccuracies nor by erroneous body weight. In addition, the most relevant improvement in SUVR over SUV is that it can reduce the variability caused by interscan variations in the input function [24]. It has been reported that SUVR exhibits a much better linear correlation with the absolute metabolic rate of glucose consumption than SUV [24]. Furthermore, increasing SUVR by 1 unit does not result in excessive increases in the odds. In the present study, lung SUVR was used to develop prediction models and showed better performance than lung SUVmax, SUVmean and SUVmin in predicting lung cancer development. In addition, prediction models using the MH index showed good performance in predicting lung cancer development. The MH index, a measure of F-18 FDG uptake heterogeneity in lung parenchyma, correlates with the extent of pulmonary inflammation and offers advantages over SUV in overcoming its limitations [25]. Spatially heterogeneous F-18 FDG uptake has been associated with heterogeneous neutrophilic infiltration in the lungs [26].

Since lung cancer screening with annual low-dose CT causes additional medical costs due to the high number of false-positive screens and harmful effects of excess radiation exposure, many lung cancer prediction models using various epidemiologic data have been proposed [27]. In addition, molecular and genetic markers have been incorporated to improve the performance of risk prediction models, although the observed gains have been mostly incremental. Spitz et al. [28] reported that the prediction models for smoking history performed better when adding two host DNA repair capacity markers (AUC = 0.68). El-Zein et al. [29] extended the prediction models using smoking history by adding a cytokinesis-blocked micronucleus assay endpoint, resulting in substantially improved prediction (AUC = 0.61–0.92). However, these risk prediction models using genetic biomarkers are still limited in practice, and modest gains in discrimination from incorporating genetic biomarkers would not outweigh the added costs [30]. Recently, Tammemagi et al. [31] developed a lung cancer risk prediction model that included low-dose CT screening results in NLST data and demonstrated good discrimination (AUC = 0.761) in external validation data from the American College of Radiology Imaging Network (ACRIN). However, there is still a limitation, as it requires results from three chest CT scans. The present study developed novel combined prediction models using metabolic parameters measured from F-18 FDG PET and clinical factors such as age, sex, smoking history, and BMI. The combined prediction model showed higher performance (AUC = 0.867 and 0.901) than the clinical model (AUC = 0.798). Other than the clinical prediction model using age, sex, smoking history, and BMI, several clinical prediction models were developed using conventional risk factors, including race/ethnicity, education, chronic obstructive pulmonary disease, history of cancer, family history of lung cancer, and asbestos exposure [30]. Thus, a prediction model combining these conventional risk factors and metabolic parameters could show better performance than the combined prediction model for lung cancer development in the present study.

There are some potential limitations in the present study. First, the study population was relatively small, based on hospital data, and was drawn only from South Korea; therefore, the results may vary in other geographic locations. In addition, the prevalence of lung cancer observed in the present study was comparatively higher than in previous studies [11]. This disparity can be attributed to the exclusion criteria employed in the present study, which specifically focused on individuals who underwent follow-up chest CT or PET/CT scans. Consequently, a significant proportion of individuals who did not undergo these follow-up scans were excluded from the control group. This limitation arose from the retrospective nature of the study and that it utilized F-18 FDG PET/CT for the health screenings. To accurately assess the performance of our predictive model, further investigations are warranted, encompassing the entire study population with comprehensive follow-up. Second, the metabolic parameters on F-18 FDG PET images were measured based on manually drawn ROIs, which might cause reproducibility

and harmonization problems in the present study. The larger three-dimensional ROI is largely affected by the interference of pulmonary vascular metabolism and the motion artifact of the lung, which may measure the metabolic parameters inaccurately [32]. In the present study, these could be measured consistently by placing small two-dimensional ROIs on the same area in each lung lobe, far enough inward from the outer pulmonary border, less affected by chest movement. Measuring metabolic parameters by automatic segmentation of lung parenchyma, excluding pulmonary nodules and vascular structures, could be used to construct a lung cancer prediction model with better accuracy and reproducibility. Furthermore, we were unable to incorporate additional environmental and genetic risk factors into the prediction model of lung cancer development in addition to the metabolic parameters. These additional factors could enhance the reliability of the present study and improve the performance of the lung cancer prediction model. Further study is needed incorporating these additional factors, to develop the lung cancer prediction models. Third, F-18 FDG PET is not routinely performed for cancer screening. However, since the prediction model that combines metabolic parameters with clinical risk factors showed high performance in predicting lung cancer development, application of the model using F-18 FDG PET might result in a reduction in the number of individuals without lung cancer who are subjected to additional and more invasive procedures to rule out a lung cancer diagnosis following a nondiagnostic bronchoscopy [30]. Even if the cancer detection rate is low on F-18 FDG PET for cancer screening [33], the benefit of F-18 FDG PET can be increased by providing additional information on lung cancer risk.

Conclusion

The metabolic parameters on F-18 FDG PET are related to an increased risk of lung cancer. The metabolic parameters on F-18 FDG PET can be used as a biomarker to provide information that is independent of clinical parameters for lung cancer risk. The prediction model that combines both clinical factors and metabolic parameters improves the predictive value for lung cancer development over the clinical model alone. Further studies with a larger number of study populations using automatic quantification of metabolic parameters on F-18 FDG PET are needed to achieve more consistent and improved results for the prediction of lung cancer development.

Supplementary Information The online version contains supplementary material available at https://doi.org/10.1007/s12149-023-01858-5.

Author contributions KC: formal analysis, methodology, writing—original draft, visualisation; JSP: data curation, conceptualization, methodology, supervision, validation; HN: methodology, writing—review and editing; SHP: methodology, visualization; HJK: formal analysis, investigation. B-IS: resources, software; HWK: data curation; formal analysis, funding acquisition, investigation, project administration, supervision, validation, writing—review and editing.

Funding This research was funded by a National Research Foundation of Korea (NRF) grant funded by the Korean government (MSIP) (Grant number: RS-2023-00243836) and by a grant of the Korea Health Technology R&D Project through the Korea Health Industry Development Institute (KHIDI), funded by the Ministry of Health & Welfare, Republic of Korea (Grant number: HI21C1074).

Availability of data and materials The datasets used and/or analyzed during the current study are available from the corresponding author on reasonable request.

Declarations

Conflict of interest No potential conflicts of interest were disclosed.

Ethical considerations Institutional Review Board approval was obtained. Written consents were obtained from all participants involved in the study.

Consent for publication Not applicable.

References

1. McGuire S. World Cancer Report 2014. Geneva, Switzerland: World Health Organization, International Agency for Research on Cancer, WHO Press, 2015. Adv Nutr. 2016;7(2):418–9. https://doi.org/10.3945/an.116.012211 (**Epub 2016/03/17. PubMed PMID: 26980827; PubMed Central PMCID: PMCPMC4785485**).
2. Force USPST, Krist AH, Davidson KW, Mangione CM, Barry MJ, Cabana M, et al. Screening for lung cancer: US preventive services task force recommendation statement. JAMA. 2021;325(10):962–70. https://doi.org/10.1001/jama.2021.1117. (**Epub 2021/03/10, PubMed PMID: 33687470**).
3. Muller DC, Johansson M, Brennan P. Lung Cancer risk prediction model incorporating lung function: development and validation in the UK Biobank prospective cohort study. J Clin Oncol. 2017;35(8):861–9. https://doi.org/10.1200/JCO.2016.69.2467. (**Epub 2017/01/18, PubMed PMID: 28095156**).
4. Bach PB, Mirkin JN, Oliver TK, Azzoli CG, Berry DA, Brawley OW, et al. Benefits and harms of CT screening for lung cancer: a systematic review. JAMA. 2012;307(22):2418–29. https://doi.org/10.1001/jama.2012.5521. (**Epub 2012/05/23, PubMed PMID: 22610500; PubMed Central PMCID: PMCPMC3709596**).
5. Conway EM, Pikor LA, Kung SH, Hamilton MJ, Lam S, Lam WL, et al. Macrophages, inflammation, and lung cancer. Am J Respir Crit Care Med. 2016;193(2):116–30. https://doi.org/10.1164/rccm.201508-1545CI. (**Epub 2015/11/20, PubMed PMID: 26583808**).
6. Landskron G, De la Fuente M, Thuwajit P, Thuwajit C, Hermoso MA. Chronic inflammation and cytokines in the tumor microenvironment. J Immunol Res. 2014;2014:149185. https://doi.org/10.1155/2014/149185. (**Epub 2014/06/06, PubMed PMID: 24901008; PubMed Central PMCID: PMCPMC4036716**).
7. Jamar F, Buscombe J, Chiti A, Christian PE, Delbeke D, Donohoe KJ, et al. EANM/SNMMI guideline for 18F-FDG use in inflammation and infection. J Nucl Med. 2013;54(4):647–58.

8. Castiaux A, Van Simaeys G, Goldman S, Bondue B. Assessment of 18F-FDG uptake in idiopathic pulmonary fibrosis: influence of lung density changes. Eur J Hybrid Imaging. 2018;2(1):27.
9. Bae SU, Won KS, Song BI, Jeong WK, Baek SK, Kim HW. Accuracy of F-18 FDG PET/CT with optimal cut-offs of maximum standardized uptake value according to size for diagnosis of regional lymph node metastasis in patients with rectal cancer. Cancer Imaging. 2018;18(1):32. https://doi.org/10.1186/s40644-018-0165-5. (**Epub 2018/09/16, PubMed PMID: 30217167; PubMed Central PMCID: PMCPMC6137872**).
10. Prakash P, Kalra MK, Sharma A, Shepard JA, Digumarthy SR. FDG PET/CT in assessment of pulmonary lymphangitic carcinomatosis. AJR Am J Roentgenol. 2010;194(1):231–6. https://doi.org/10.2214/AJR.09.3059. (**Epub 2009/12/24, PubMed PMID: 20028927**).
11. Bailly C, Bodet-Milin C, Bourgeois M, Gouard S, Ansquer C, Barbaud M, et al. Exploring tumor heterogeneity using PET imaging: the big picture. Cancers (Basel). 2019. https://doi.org/10.3390/cancers11091282. (**Epub 2019/09/05, PubMed PMID: 31480470; PubMed Central PMCID: PMCPMC6770004**).
12. Park S, Nam BH, Yang HR, Lee JA, Lim H, Han JT, et al. Individualized risk prediction model for lung cancer in Korean men. PLoS ONE. 2013;8(2):e54823. https://doi.org/10.1371/journal.pone.0054823. (**Epub 2013/02/15, PubMed PMID: 23408946; PubMed Central PMCID: PMCPMC3567090**).
13. Bae K, Shim H, Tao C, Chang S, Wang J, Boudreau R, et al. Intra-and inter-observer reproducibility of volume measurement of knee cartilage segmented from the OAI MR image set using a novel semi-automated segmentation method. Osteoarthr Cartil. 2009;17(12):1589–97.
14. Arkes HR, Dawson NV, Speroff T, Harrell FE Jr, Alzola C, Phillips R, et al. The covariance decomposition of the probability score and its use in evaluating prognostic estimates. SUPPORT Investigators. Med Decisi Mak Int J Soc Med Decis Mak. 1995;15(2):120–31.
15. Hecht SS. Progress and challenges in selected areas of tobacco carcinogenesis. Chem Res Toxicol. 2008;21(1):160–71. https://doi.org/10.1021/tx7002068. (**Epub 2007/12/07, PubMed PMID: 18052103; PubMed Central PMCID: PMCPMC2556958**).
16. Engels EA. Inflammation in the development of lung cancer: epidemiological evidence. Expert Rev Anticancer Ther. 2008;8(4):605–15. https://doi.org/10.1586/14737140.8.4.605. (**Epub 2008/04/12, PubMed PMID: 18402527**).
17. de Prost N, Tucci MR, Melo MF. Assessment of lung inflammation with 18F-FDG PET during acute lung injury. AJR Am J Roentgenol. 2010;195(2):292–300. https://doi.org/10.2214/AJR.10.4499. (**Epub 2010/07/24, PubMed PMID: 20651183; PubMed Central PMCID: PMCPMC3172046**).
18. Chen DL, Bedient TJ, Kozlowski J, Rosenbluth DB, Isakow W, Ferkol TW, et al. [18F]fluorodeoxyglucose positron emission tomography for lung antiinflammatory response evaluation. Am J Respir Crit Care Med. 2009;180(6):533–9. https://doi.org/10.1164/rccm.200904-0501OC. (**Epub 2009/07/04, PubMed PMID: 19574441; PubMed Central PMCID: PMCPMC2742744**).
19. Sugawara Y, Zasadny KR, Neuhoff AW, Wahl RL. Reevaluation of the standardized uptake value for FDG: variations with body weight and methods for correction. Radiology. 1999;213(2):521–5. https://doi.org/10.1148/radiology.213.2.r99nv37521. (**Epub 1999/11/07, PubMed PMID: 10551235**).
20. Freedman NM, Sundaram SK, Kurdziel K, Carrasquillo JA, Whatley M, Carson JM, et al. Comparison of SUV and Patlak slope for monitoring of cancer therapy using serial PET scans. Eur J Nucl Med Mol Imaging. 2003;30(1):46–53. https://doi.org/10.1007/s00259-002-0981-4. (**Epub 2002/12/17, PubMed PMID: 12483409**).
21. Sadato N, Tsuchida T, Nakaumra S, Waki A, Uematsu H, Takahashi N, et al. Non-invasive estimation of the net influx constant using the standardized uptake value for quantification of FDG uptake of tumours. Eur J Nucl Med. 1998;25(6):559–64.
22. Chen W, Dilsizian V. PET assessment of vascular inflammation and atherosclerotic plaques: SUV or TBR? J Nucl Med. 2015;56(4):503–4. https://doi.org/10.2967/jnumed.115.154385. (**Epub 2015/02/28, PubMed PMID: 25722451**).
23. van den Hoff J, Oehme L, Schramm G, Maus J, Lougovski A, Petr J, et al. The PET-derived tumor-to-blood standard uptake ratio (SUR) is superior to tumor SUV as a surrogate parameter of the metabolic rate of FDG. EJNMMI Res. 2013;3(1):1–8.
24. Aulakh GK, Kaur M, Brown V, Ekanayake S, Khan B, Fonge H. Quantification of regional murine ozone-induced lung inflammation using [18 F] F-FDG microPET/CT imaging. Sci Rep. 2020;10(1):1–8.
25. Costa EL, Musch G, Winkler T, Schroeder T, Harris RS, Jones HA, et al. Mild endotoxemia during mechanical ventilation produces spatially heterogeneous pulmonary neutrophilic inflammation in sheep. Anesthesiology. 2010;112(3):658–69. https://doi.org/10.1097/ALN.0b013e3181cbd1d4. (**Epub 2010/02/25, PubMed PMID: 20179503; PubMed Central PMCID: PMCPMC2829720**).
26. Bach PB, Kattan MW, Thornquist MD, Kris MG, Tate RC, Barnett MJ, et al. Variations in lung cancer risk among smokers. J Natl Cancer Inst. 2003;95(6):470–8.
27. Spitz MR, Hong WK, Amos CI, Wu X, Schabath MB, Dong Q, et al. A risk model for prediction of lung cancer. J Natl Cancer Inst. 2007;99(9):715–26. https://doi.org/10.1093/jnci/djk153. (**Epub 2007/05/02, PubMed PMID: 17470739**).
28. Spitz MR, Etzel CJ, Dong Q, Amos CI, Wei Q, Wu X, et al. An expanded risk prediction model for lung cancer. Cancer Prev Res (Phila). 2008;1(4):250–4. https://doi.org/10.1158/1940-6207.CAPR-08-0060. (**Epub 2009/01/14, PubMed PMID: 19138968; PubMed Central PMCID: PMCPMC2854404**).
29. El-Zein RA, Lopez MS, D'Amelio AM, Liu M, Munden RF, Christiani D, et al. The cytokinesis-blocked micronucleus assay as a strong predictor of lung cancer: extension of a lung cancer risk prediction model. Cancer Epidemiol Prev Biomark. 2014;23(11):2462–70.
30. Sakoda LC, Henderson LM, Caverly TJ, Wernli KJ, Katki HA. Applying risk prediction models to optimize lung cancer screening: current knowledge, challenges, and future directions. Curr Epidemiol Rep. 2017;4(4):307–20. https://doi.org/10.1007/s40471-017-0126-8. (**Epub 2018/03/14, PubMed PMID: 29531893; PubMed Central PMCID: PMCPMC5844483**).
31. Tammemägi MC, Ten Haaf K, Toumazis I, Kong CY, Han SS, Jeon J, et al. Development and validation of a multivariable lung cancer risk prediction model that includes low-dose computed tomography screening results: a secondary analysis of data from the National lung screening trial. JAMA Netw Open. 2019;2(3):e190204-e.
32. Ziai P, Hayeri MR, Salei A, Salavati A, Houshmand S, Alavi A, et al. Role of optimal quantification of FDG PET imaging in the clinical practice of radiology. Radiographics. 2016;36(2):481–96. https://doi.org/10.1148/rg.2016150102. (**Epub 2016/03/11, PubMed PMID: 26963458**).
33. Lee JW, Kang KW, Paeng JC, Lee SM, Jang SJ, Chung J-K, et al. Cancer screening using 18 F-FDG PET/CT in Korean asymptomatic volunteers: a preliminary report. Ann Nucl Med. 2009;23(7):685–91.